

FACULDADE DE ENGENHARIA DA UNIVERSIDADE DO PORTO

Optimization of an airplane wing representative structure for vibration and buckling

Tiago António da Silva Soares



Dissertation submitted to Faculdade de Engenharia da Universidade do Porto for the
degree of:
Master in Mechanical Engineering

Supervisor: Carlos Alberto Conceição António (Cathedral professor)

Co-supervisor: Pedro Manuel Leal Ribeiro (Associate professor)

Porto, October 2022

Optimization of an airplane wing representative structure for vibration and buckling

Tiago António da Silva Soares

Dissertation submitted to Faculdade de Engenharia da Universidade do
Porto for the degree of:
Master in Mechanical Engineering

Porto, October 2022

Abstract

The design of composite structures for the aerospace industry is a multidisciplinary task, involving several coupled domains, which increases significantly the development time. Besides that, the necessity to comply with too many requirements in order to establish the system's performance makes that design even more complicated. The aerospace industry has strict rules regarding the design of those structures, mainly because they are high-responsibility applications. Therefore, each individual design must be validated by suitable tests, which are, normally, time-consuming. Multidisciplinary optimization procedures became an alternative over time, because they are capable of considering several domains simultaneously and the interaction between them as well, satisfying design constraints taking into account one or more objectives.

In this report, an airplane wing representative structure provided by the Cardiff School of Engineering is scrutinized. An evolutionary-based algorithm, genetic one, is applied in order to maximise the fundamental natural frequency and the critical buckling load of the representative structure, under several prescribed constraints and altering only the plies' orientations or thicknesses. An artificial neural network is used to predict the output values necessary for the application and development of the genetic algorithm, reducing the number of FEM simulations needed, using Abaqus[®] software. The genetic procedure is used both for optimising the ANN's configuration and to achieve the desired maximised ω_1 or P_{crit} value.

Firstly, the structure is optimised regarding its fundamental natural frequency, ω_1 , by changing the plies' orientations and afterwards adding the thicknesses as design variables. The structure's vibration amplitude may excessively increase if the excitation frequencies are close to the important ones in the excitation spectrum, particularly for lower-damping structures, which may damage other components or even cause human casualties. The maximisation of the first natural frequency of vibration is a means of avoiding this issue when the first mode of vibration dominates the response. For each individual optimization procedure, the relative importance of each design variable on the variance of the output response is calculated based on the first order *Sobol* indices. Moreover, an analytical approach based on the *Rayleigh-Ritz* method is provided in order to predict the natural frequencies of the composite stiffened panel.

Due to the unpredictability of a certain structure post-buckling, the airplane wing representative structure is also optimised with regard to its critical buckling load. Therefore, the structure's loading spectrum can be enlarged without compromising its performance and safety. The plies' angles and thicknesses of the composite panel are conveniently modified. Furthermore, the linear aggregation method is used to consider the minimisation of the structure's weight as an additional objective. The *Lévy's* method is applied to formulate an approach capable of determining the buckling loads of a composite panel, owing to its ease of implementation.

Keywords: Composite laminate, Artificial neural network, Uniform design method, Genetic algorithm, Fundamental natural frequency, Critical buckling load.

Resumo

O projeto de estruturas compósitas para a indústria aeroespacial é uma tarefa multidisciplinar, envolvendo vários domínios acoplados, o que aumenta significativamente o tempo de desenvolvimento. Além disso, a necessidade de cumprir com muitos requisitos para estabelecer o desempenho do sistema torna esse projeto ainda mais complicado. A indústria aeroespacial possui regras rígidas no que diz respeito ao projeto dessas estruturas, principalmente por se tratarem de aplicações de alta responsabilidade. Conseqüentemente, cada projeto individual deve ser validado por testes adequados, que são, normalmente, demorados. Procedimentos de otimização multidisciplinar tornaram-se uma alternativa ao longo do tempo, por serem capazes de considerar vários domínios simultaneamente assim como a interação entre eles, satisfazendo diversas restrições de projeto tendo em consideração um ou mais objetivos.

Neste documento analisa-se uma estrutura representativa de uma asa de um avião fornecida pela *Cardiff School of Engineering*. Um algoritmo baseado na evolução, algoritmo genético, é aplicado com o objetivo de maximizar a frequência natural fundamental e a carga crítica de encurvadura da estrutura representativa, sob várias restrições pré-estabelecidas e alterando apenas as orientações e espessuras das camadas de material compósito. Uma rede neuronal artificial é usada para obter os valores de saída necessários à aplicação e desenvolvimento do algoritmo genético, reduzindo o número de simulações de elementos finitos através do *software* Abaqus®. O procedimento baseado na genética é usado quer para otimizar a estrutura da rede neuronal quer para obter o valor maximizado desejado, ω_1 ou P_{crit} , conforme o problema.

Primeiramente, a estrutura é otimizada no que diz respeito à sua frequência natural fundamental, ω_1 , através da mudança das orientações das camadas e, de seguida, acrescentando as espessuras como variáveis de projeto. A amplitude de vibração da estrutura pode aumentar consideravelmente se as frequências de excitação forem próximas de frequências importantes no espectro de excitação, particularmente para estruturas de baixo amortecimento, o que pode danificar outras estruturas adjacentes ou até causar falhas humanas. A importância relativa de cada variável de projeto na variância da variável de saída é expressa através dos índices de *Sobol* de primeira ordem para cada procedimento de otimização realizado. Adicionalmente, um procedimento analítico baseado no método de *Rayleigh-Ritz* foi desenvolvido com o objetivo de obter as frequências naturais do painel compósito com reforços longitudinais de alumínio.

O comportamento de uma certa estrutura pós-encurvadura é completamente imprevisível, sendo acompanhada por mudanças de rigidez, logo a sua otimização em relação à carga crítica de encurvadura é também de extrema importância. Assim, o espectro de cargas admissível para a estrutura pode ser alargado sem comprometer o seu desempenho e segurança. As orientações e espessuras das camadas do painel compósito são convenientemente modificadas. O método da agregação linear é usado a fim de considerar a minimização do peso da estrutura como um objetivo adicional. O método de *Lévy* é aplicado com o objetivo de formular um procedimento analítico capaz de determinar as cargas de encurvadura de um painel compósito, devido à sua facilidade de

implementação.

Keywords: Laminado compósito, Rede neuronal artificial, *Uniform Design Method*, Algoritmo genético, Frequência natural fundamental, Carga crítica de encurvadura.

Acknowledgements

This thesis was written as part of the COST action CA18203, "Optimising Design for Inspection", which has been supported by the Horizon 2020 framework initiative of the European Union. In addition, I want to express my gratitude to everyone who contributed to making the present report feasible:

- To Prof. Carlos Conceição António for sharing his knowledge, availability and motivation to always improve on my work;
- To Prof. Pedro Leal Ribeiro for the theme suggestion and for his prompt support;
- To all COST action members who made a contribution to the development of the current work;
- To my friends at FEUP, particularly André Ramos, Guilherme Tavares, João Pedro Alves and Rúben Araújo, for the companionship over these 5 years, helping me to grow both personally and professionally;
- To my family, especially my parents, for their unconditional support.

Tiago Soares

This article/publication is based upon work from COST Action 18203—Optimized Design for Inspection (ODIN), supported by COST (European Cooperation in Science and Technology). COST (European Cooperation in Science and Technology) is a funding agency for research and innovation networks. Our Actions help connect research initiatives across Europe and enable scientists to grow their ideas by sharing them with their peers. This boosts their research, career and innovation.

www.cost.eu



*“The only true wisdom
is in knowing you know nothing.”*

Socrates

Contents

1	Introduction	1
1.1	Background and motivation	1
1.2	Optimising design for inspection	4
1.3	Objectives	5
1.4	Thesis layout	6
2	State of the art	7
2.1	Introduction	7
2.2	Optimization algorithms and machine learning	7
2.3	Optimization algorithms: ANN's	11
2.3.1	Description	11
2.3.2	How ANN's work	11
2.3.3	Composition	12
2.3.4	Applications	14
2.3.5	Advantages and disadvantages	14
2.3.6	Training process	15
2.4	Gradient-based optimization algorithms	18
2.4.1	Mathematical model	19
2.4.2	Optimised versions of the backpropagation algorithm	21
2.4.3	Optimization of composite structures using gradient-based methods	21
2.5	Evolutionary-based optimization algorithms	24
2.6	Genetic algorithms	26
2.6.1	Fitness function definition	28
2.6.2	Methods to include the problem constraints based on genetic algorithms	29
2.6.3	Selection operator	29
2.6.4	Crossover operator	30
2.6.5	Mutation operator	30
2.6.6	Convergence and stopping criteria	31
2.6.7	Guidelines to achieve a good performance	31
2.6.8	Optimization of composite structures using evolutionary-based algorithms	32
2.7	Multi-objective optimization	35
2.7.1	Multi-objective optimization methods	36
2.7.2	Multi-objective optimization classification	36
2.7.3	Constraint multi-objective evolutionary algorithms	39
2.7.4	Multi-objective optimization applied to composite structures	40
2.8	Design of composite structures	42
2.9	Summary	43
3	Mathematical model	45

3.1	Introduction	45
3.2	Composite materials	45
3.3	Equations of motion for an unstiffened composite plate	49
3.3.1	<i>Hamilton's</i> variational principle	49
3.3.2	Equations of motion	50
3.4	Calculation of the mechanical responses	52
3.4.1	Natural frequencies	52
3.4.2	Buckling loads	54
3.4.3	Derivation of the differential equations of motion for a stiffened composite plate	56
3.5	Finite Element Method	59
3.6	Final remarks	59
4	Wing representative structure's description	61
4.1	Introduction	61
4.2	Wing representative structure's geometry	61
4.3	Elastic materials	62
4.4	Finite element method	63
4.5	Final remarks	65
5	Optimization of the airplane wing representative structure for vibration	67
5.1	Introduction	67
5.2	Description of the optimization algorithm	68
5.2.1	Uniform Design Method	70
5.2.2	ANN model development	70
5.2.3	Optimal design procedure	72
5.2.4	Genetic algorithm description	73
5.2.5	Global sensitivity analysis	74
5.3	Fundamental natural frequency: ply angles	76
5.3.1	Design of experiments	76
5.3.2	Modes of vibration	80
5.3.3	ANN learning procedure	85
5.3.4	Optimization of the ply angles	91
5.3.5	<i>Sobol</i> indices	93
5.3.6	Conclusions	94
5.4	Fundamental natural frequency: ply angles and thicknesses	95
5.4.1	Design of experiments	95
5.4.2	ANN learning procedure	97
5.4.3	Optimization of the layers' orientations and thicknesses	103
5.4.4	<i>Sobol</i> indices	105
5.4.5	Conclusions	106
5.5	Final remarks	107
6	Optimization of the airplane wing representative structure for buckling	109
6.1	Design of experiments	110
6.2	ANN learning procedure	112
6.3	Optimization of the layers' orientations and thicknesses	117
6.4	<i>Sobol</i> indices	121
6.5	Conclusions and final remarks	122

7	Conclusions and Future Work	123
7.1	Conclusions	123
7.2	Further Work	124
	References	127

List of Figures

Figure 1.1-	Airplane wing representative structure. Adapted from [15].	5
Figure 2.1-	Simple ANN's configuration.	12
Figure 2.2-	ANN's main architecture.	13
Figure 2.3-	Gaussian function. Adapted from [19].	14
Figure 2.4-	Different ways of data generalisation [55].	18
Figure 2.5-	Multilayer perceptron network. Adapted from [19].	19
Figure 2.6-	Multi-objective optimization methods. Adapted from [29, 90, 92]. . . .	36
Figure 3.1-	Material principal directions.	46
Figure 3.2-	Representation of the membrane forces and moments acting on the composite panel.	50
Figure 4.1-	Airplane wing representative structure and its components. Provided by Cardiff School of Engineering.	61
Figure 4.2-	SC8R and C3D8I elements: linear degrees of freedom.	65
Figure 4.3-	Stiffened composite plate's mesh.	65
Figure 5.1-	Analysed substructure of the airplane wing representative structure. . . .	67
Figure 5.2-	Flow diagram of the optimization framework. Adapted from [124–126].	69
Figure 5.3-	ANN learning and optimization procedure. Adapted from [124–126]. . .	72
Figure 5.4-	Genetic algorithm's description. Adapted from [124–126].	74
Figure 5.5-	Stacking sequence and design variables for the optimization of ω_1	76
Figure 5.6-	3D representation of the experimental points.	79
Figure 5.7-	Representation of the experimental points in the three mutually orthogonal planes.	79
Figure 5.8-	Scatter plot of ω_1 , having the plies orientations as design variables. . . .	80
Figure 5.9-	Vibration mode shapes of the composite panel for the lower fundamental natural frequency value.	82
Figure 5.10-	Vibration mode shapes of the composite panel for the intermediate fundamental natural frequency value.	83
Figure 5.11-	Vibration mode shapes of the composite panel for the higher fundamental natural frequency value.	84
Figure 5.12-	Evolution of the ANN's absolute error over the generations, created to predict ω_1 , having the plies orientations as design variables.	86
Figure 5.13-	Evolution of the ANN's relative error over the generations, created to predict ω_1 , having the plies orientations as design variables.	87
Figure 5.14-	Comparison between the ANN and FEM results for the training dataset of the ANN created to predict ω_1 , having the plies orientations as design variables.	88

Figure 5.15-	Evolution of the maximised fundamental natural frequency over the generations, having the plies orientations as design variables.	92
Figure 5.16-	<i>Sobol</i> indices corresponding to the ω_1 maximisation, having the plies orientations as design variables	94
Figure 5.17-	Stacking sequence and design variables for the optimization of ω_1 , including the plies thicknesses.	95
Figure 5.18-	Scatter plot of ω_1 , having the plies orientations and thicknesses as design variables.	98
Figure 5.19-	Evolution of the ANN's absolute error over the generations, created to predict ω_1 , having the plies orientations and thicknesses as design variables.	99
Figure 5.20-	Evolution of the ANN's relative error over the generations, created to predict ω_1 , having the plies orientations and thicknesses as design variables.	99
Figure 5.21-	Comparison between the ANN and FEM results for the training dataset of the ANN created to predict ω_1 , having the plies orientations and thicknesses as design variables.	101
Figure 5.22-	Evolution of the maximised fundamental natural frequency over the generations, having the layers orientations and thicknesses as design variables.	104
Figure 5.23-	<i>Sobol</i> indices corresponding to the ω_1 maximisation, having the plies orientations and thicknesses as design variables.	106
Figure 6.1-	Stacking sequence and design variables for the optimization of P_{crit} , including the plies thicknesses.	109
Figure 6.2-	FEM model for the critical buckling load prediction.	110
Figure 6.3-	Scatter plot of P_{crit}	112
Figure 6.4-	Evolution of the ANN's absolute error over the generations, created to predict P_{crit} , having the plies orientations and thicknesses as design variables.	113
Figure 6.5-	Evolution of the ANN's relative error over the generations, created to predict P_{crit} , having the plies orientations and thicknesses as design variables.	113
Figure 6.6-	Comparison between the ANN and FEM results for the training dataset of the ANN created to predict P_1 , having the plies orientations and thicknesses as design variables.	114
Figure 6.7-	Evolution of the maximised critical buckling load over the generations, having the plies orientations and thicknesses as design variables.	120
Figure 6.8-	<i>Sobol</i> indices corresponding to the P_{crit} maximisation, having the plies orientations and thicknesses as design variables.	122

List of Tables

Table 2.1-	Performance of the gradient-based backpropagation algorithm. Adapted from [19, 20, 25].	22
Table 2.2-	Biology-inspired algorithms: advantages and disadvantages. Adapted from [17, 26, 27, 31–35].	25
Table 2.3-	Physics-inspired algorithms: advantages and disadvantages. Adapted from [17, 26, 70, 71].	26
Table 2.4-	Properties of prepreg composite materials. Adapted from [74].	28
Table 2.5-	Crossover operators. Adapted from [29].	31
Table 4.1-	List of items and their materials.	62
Table 4.2-	Elastic properties of the adhesive and aluminium alloys.	62
Table 4.3-	Elastic properties of USN150B.	63
Table 5.1-	Uniform design table, $L_{27}(3^{10})$	77
Table 5.2-	Accessory table, $L_{27}(3^{10})$	77
Table 5.3-	Experimental points for the optimization of ω_1 , having the plies orientations as design variables.	78
Table 5.4-	Ratios between the extreme transverse displacements values of the natural vibration shapes.	80
Table 5.5-	Comparison between the ANN and FEM results for the training dataset of the ANN created to predict ω_1 , having the plies orientations as design variables.	87
Table 5.6-	Comparison between the ANN and FEM results for the training dataset of the ANN created to predict ω_2 , having the plies orientations as design variables.	88
Table 5.7-	Influence of the number of hidden nodes on the absolute and relative errors of the ANN learning procedure.	89
Table 5.8-	Influence of the range of weights at the hidden-output interconnection on the absolute and relative errors of the ANN learning procedure.	89
Table 5.9-	Influence of the population's dimension on the absolute and relative errors of the ANN learning procedure.	90
Table 5.10-	Influence of the mechanism of diversity control on the absolute and relative errors of the ANN learning procedure.	90
Table 5.11-	Influence of the mutation percentage on the absolute and relative errors of the ANN learning procedure.	90
Table 5.12-	Optimised laminate configuration for vibration, considering the layers' orientations as design variables.	92
Table 5.13-	Influence of the allowable θ_1 range on the maximised obtained value for the fundamental natural frequency.	93

Table 5.14-	<i>Sobol</i> indices regarding the optimization of the structure for vibration, having only the plies orientations as design variables.	93
Table 5.15-	Uniform design table, $L_{27}(27^{11})$	96
Table 5.16-	Accessory table, $L_{27}(27^{11})$	96
Table 5.17-	Experimental points for the optimization of ω_1 , having the plies orientations and thicknesses as design variables.	97
Table 5.18-	Comparison between the ANN and FEM results for the training dataset of the ANN created to predict ω_1 , having the plies orientations and thicknesses as design variables.	100
Table 5.19-	Comparison between the ANN and FEM results for the training dataset of the ANN created to predict ω_2 , having the plies orientations and thicknesses as design variables.	100
Table 5.20-	Influence of the number of hidden nodes on the absolute and relative errors of the ANN learning procedure.	101
Table 5.21-	Influence of the range of weights at the hidden-output interconnection on the absolute and relative errors of the ANN learning procedure.	102
Table 5.22-	Influence of the population's dimension on the absolute and relative errors of the ANN learning procedure.	102
Table 5.23-	Influence of the mechanism of diversity control on the absolute and relative errors of the ANN learning procedure.	102
Table 5.24-	Influence of the elite percentage on the absolute and relative errors of the ANN learning procedure.	103
Table 5.25-	Optimised laminate configuration for vibration, considering the layers' orientations and thicknesses as design variables.	103
Table 5.26-	Optimised laminate configuration for vibration, considering the layers orientations and thicknesses as design variables: other configuration.	104
Table 5.27-	Comparison between the total panel's thickness for each optimised configuration for vibration, having the plies orientations and thicknesses as design variables	105
Table 5.28-	<i>Sobol</i> indices regarding the optimization of the structure for vibration, having the plies orientations and thicknesses as design variables.	105
Table 6.1-	Experimental points for the optimization of P_{crit} , having the plies orientations and thicknesses as design variables.	111
Table 6.2-	Comparison between the ANN and FEM results for the training dataset of the ANN created to predict P_1 , having the plies orientations and thicknesses as design variables.	114
Table 6.3-	Comparison between the ANN and FEM results for the training dataset of the ANN created to predict P_2 , having the plies orientations and thicknesses as design variables.	115
Table 6.4-	Influence of the number of hidden nodes on the absolute and relative errors of the ANN learning procedure.	115
Table 6.5-	Influence of the range of weights at the hidden-output interconnection on the absolute and relative errors of the ANN learning procedure.	116
Table 6.6-	Influence of the population's dimension on the absolute and relative errors of the ANN learning procedure.	116
Table 6.7-	Influence of the mechanism of diversity control on the absolute and relative errors of the ANN learning procedure.	117

Table 6.8-	Optimised laminate configuration for buckling, considering the layers orientations and thicknesses as design variables.	120
Table 6.9-	Optimised laminate configuration for buckling considering the other well fitted configuration.	121
Table 6.10-	<i>Sobol</i> indices regarding the optimization of the structure for buckling, having the plies orientations and thicknesses as design variables.	121

List of symbols

Abbreviations

ACO	Ant Colony Optimization
AI	Artificial Intelligence
ANN	Artificial Neural Network
AFP	Automated Fibre Placement
BSA	Backtracking Search Algorithm
BFO	Bacterial Foraging Optimization
BCA	Bee Colony Algorithm
BRKGA	Biassed Random Key Genetic Algorithm
BB-BC	Big Bang-Big Crunch
BBD	Box Behnken Design
CFRP	Carbon Fiber Reinforced Polymer
CCD	Central Composite Design
CFO	Central Force Optimizer
CBGA	Centre Based Genetic Algorithm
CSS	Charged System Search
CAD	Computer-Aided Design
CNN	Convolutional Neural Network
CSA	Cuckoo Search Algorithm
DM	Data Mining
DMT	Data Mining Technology
DL	Deep Learning
EP	Enlarged Population
COST	European Cooperation in Science and Technology
FEM	Finite Element Method
FA	Firefly Algorithm
FORM	First Order Reliability Method
FFD	Full Factorial Design
GbSA	Galaxy-based Search Algorithm
GA	Genetic Algorithm
GSA	Global Sensitivity Analysis
GSA	Gravitational Search Algorithm
HSA	Harmony Search Algorithm
ICA	Independent Component Analysis
LOA	Layerwise Optimization Approach

LSA	L ightning S earch A lgorithm
ML	M achine L earning
MAC	M odal A ssurance C riterion
MCS	M onte C arlo S imulation
MPP	M ost P robable F ailure P oint
MDO	M ulti- D isciplinary O ptimization
MOGA	M ulti- O bjective G enetic A lgorithm
MOHGA	M ulti- O bjective H ierarchical G enetic A lgorithm
NDI	N on- D estructive I nspection
NSGA	N on- D ominated S orting G enetic A lgorithm
NTM	N umber- T heoretic M ethod
OAD	O rthogonal A rray D esign
PSO	P article S warm O ptimization
PWAS	P iezoelectric W afer A ctive S ensor
PCA	P rincipal C omponent A nalysis
RNN	R ecurrent N eural N etwork
RE	R elative E rror
RPSOLC	R epulsive P article S warm O ptimization with L ocal S earch and C haotic P er- turbation
RMSE	R oot- M ean- S quare E rror
SORM	S econd O rders R eliability M ethod
SA	S imulated A nnealing
SP	S mall P opulation
SHM	S tructural- H ealth M onitoring
SVM	S upport V ector M achine
UD	U niform D esign
UDM	U niform D esign M ethod
VCH	V iolation C onstraint- H andling

General Notation

a, A	Scalar (italic)
$\mathbf{a}, \{\bullet\}$	Vector (bold + lowercase)
$\mathbf{A}, [\bullet]$	Second-order tensor (bold + uppercase)

Operators

$\dot{(\bullet)}$	$d(\bullet)/d(\bullet)$	First total time derivative
$\ddot{(\bullet)}$	$d^2(\bullet)/d(\bullet)^2$	Second total time derivative
$\partial(\bullet)/\partial(\bullet)$		Partial derivative
$\nabla(\bullet)$		Gradient operator
$\sum(\bullet)$		Summation operator
$\det(\bullet) = [\bullet] $		Determinant
$\delta(\bullet)$		First variation/Virtual quantity
$(\bullet) \cdot (\bullet)$		Single contraction / dot product between two tensors
$\int_l (\bullet) dl$		Integral
$\iint_A (\bullet) dA$		Double integral
$\text{var}\langle (\bullet) \rangle$		Variance
$\text{var}\langle E \langle (\bullet) (\bullet) \rangle \rangle$		Variance of the conditional expectation

Greek Symbols

Γ	Boundary of the plate
Ω_0	Continuum domain
λ_{crit}	Critical load factor
ε	Damping ratio
ρ	Density
μ	Dynamic amplification factor
σ_y	Elastic limit stress
Γ_{error}	Error component associated to the biases
ϕ_X	Experimentally-measured mode shape
λ_{fix}	Fixed values vector
β	Frequency ratio
ω_i	i^{th} natural frequency
θ_i	i^{th} ply orientation variable
η	Learning rate of the backpropagation algorithm
ε_i	Limit value assigned to the i^{th} transformed objective
α	Momentum rate of the backpropagation algorithm
ε, η	Natural coordinates
ε	Normal deformation
σ	Normal stress
κ	Parameter of the gaussian function
β_h	Parameter of the hyperbolic tangent function
α, β	Parameters relative to the <i>Jacobi</i> polynomials
ϕ_j	Particular constraint
ν	Poisson ratio
λ_i	Roots of the characteristic function
ψ	Shape function
γ	Shear deformation
τ	Shear stress
β_{sig}	Slope of the sigmoidal function curve at its inflection point
ϕ_A	Theoretically-predicted mode shape
Π	Total energy of the stiffened plate
$\boldsymbol{\varepsilon}_0^b$	Vector of curvatures at the middle surface
$\boldsymbol{\varepsilon}_0^m$	Vector of membrane strains at the middle surface
μ_i	Weight assigned to the i^{th} objective

Latin Symbols

E_{abs}	Absolute error resulted from the training procedure
u	Activation potential
\mathbf{p}_{opt}^{ANN}	ANN configuration resulted from the optimization procedure
T_i	Aspiration level assigned to the i^{th} objective
B_{ij}	Bending-extensional stiffness coefficient
M	Bending or twisting moment
D_{ij}	Bending stiffness coefficient
b_i	Bias associated to input node i
$\mathbf{r}^{(L)}$	Bias vector associated to the neurons of layer L

\mathbf{f}	Body forces vector
A_i, B_i, C_i	Coefficients which weight each shape function relative to a certain displacement
c	Compressive
P_{crit}	Critical buckling load
d_{crit}	Critical displacement
\mathbf{d}	Desired output vector
N_{pop}	Dimension of the population
m, n	Director cosines
u, v, w	Displacement components
\mathbf{u}	Displacement vector
q_b	Distributed force per unit area at the bottom of the panel
q	Distributed force per unit area at the panel
q_t	Distributed force per unit area at the top of the panel
E	Error function
A_{ij}	Extensional stiffness coefficient
$FIT^{(2)}$	Fitness function associated to the physical variable maximisation
$FIT^{(1)}$	Fitness function for the optimization of the ANN configuration
$\mathcal{P}\mathbf{F}^*$	Front of Pareto
U, V, W	Functions representative of the deformed shape of the plate
i, j, k, l, m, n	General indices
k	Index assigned to each composite lamina
dA	Infinitesimal surface element
dV	Infinitesimal volume element
h_i	i^{th} ply thickness variable
$P_n^{(\alpha, \beta)}(l)$	<i>Jacobi</i> polynomial of order n
T	Kinetic energy
L	Length of the composite panel
d_{min}, d_{max}	Limit values of a certain variable
R	Linear aggregator
m	Mass
\mathbf{M}	Mass matrix
N_{gen}	Maximum number of generations
t_c	Maximum number of random variables associated to a specific design table
N	Membrane force
$LIMDIF$	Minimum number of equal genes/variables between two different individuals selected from the population capable of taking one out from the population
MAC	Modal Assurance Criterion
I	Moment of inertia
p_n	Natural number which depends upon the number of experiments
\mathbf{d}_k	Nodal displacement vector
X, Y, Z	Normal strength
\bar{S}_i^O	Normalised Sobol index associated to each variable x_i
\bar{d}_k	Normalised value of a certain variable

C_0	Number of central points
N_r	Number of combinations of a fixed and a sample matrix values
n_L	Number of composite layers
n_{exp}	Number of experiments
s	Number of factors
n_e	Number of finite elements
N_f	Number of fixed values
INP	Number of input nodes
INT	Number of intermediate/hidden nodes
n	Number of nodes
n_{nod}	Number of nodes of each particular finite element
OUT	Number of output nodes
N	Number of repetitions of the optimization procedure
N_{stiff}	Number of stiffeners
k_{sub}	Number of subpopulations
B	Offspring group
y_j	Output value associated to node j
c	Parameter of the gaussian function
F_i, F_{ij}, F_{ijk}	Parameters related to the lamina strengths in the principal directions
P_{dist}	Parameter which defines the metric used to quantify the distance between the reference point and the admissible region of the search space
\mathbf{x}^*	Pareto optimal
$P^{(t)}$	Population of solutions for each t -generation of the first genetic algorithm
$X^{(t)}$	Population of solutions for each t -generation of the second genetic algorithm
p	Pressure acting on the composite panel
d_N^{min}, d_N^{max}	Range of normalisation
d_k	Real value of a certain variable before normalisation
\bar{Q}_{ij}	Reduced stiffness coefficient
\mathbf{z}	Reference point for multi-objective optimization
\mathbf{x}^0	Reference position vector
RE	Relative error
E_{rel}	Relative error resulted from the training procedure
$RMSE$	Root-mean-square error
\mathbf{J}_α	Sample matrix
\mathcal{P}^*	Set of Pareto's optimals
N_k	Shape function related to node k
G	Shear modulus
S	Shear strength
S_i^O	Sobol index associated to each variable x_i
\mathbf{S}	Space of admissible solutions
y_s	Spatial localization of a stiffener along the Oy axis
Q_{ij}	Stiffness coefficient
\mathbf{K}	Stiffness matrix
U_s	Strain energy
U_0	Strain energy per unit volume

t	Tensile
t_{ply}	Thickness of each ply of the panel provided by Cardiff School of Engineering
t	Time
$\hat{\mathbf{t}}$	Tractions vector acting on panel's surface
U	Uniform probability distribution function
$c_1, c_2, c_3, k^1, k^2, \alpha_j$	User-defined constants
x_i	Value of the i^{th} input node
\mathbf{x}	Vector of design variables
\mathbf{f}	Vector of objectives
$\delta \mathbf{u}$	Virtual displacement vector
$\mathbf{W}_{ji}^{(L)}$	Weight matrix whose elements denote the value of the synaptic weight that connects the j^{th} neuron of layer (L) to the i^{th} neuron of layer ($L - 1$)
w_{ij}	Weight value between nodes i and j
$\mathbf{y}_j^{(L)}$	Weight vector whose elements denote the output value related to the j^{th} neuron of layer (L)
$\mathbf{i}_j^{(L)}$	Weight vector whose elements denote the weighted input value related to the j^{th} neuron of layer (L)
$A(l)$	Weighting function
b	Width of the composite panel
F	Work done by external forces
E	Young modulus

Chapter 1

Introduction

1.1 Background and motivation

Over time, the need to develop lighter and more mechanically efficient aircraft structures led to an evolution in the structural materials used from the metals, such as steel, aluminium and titanium to composite and hybrid materials. Advanced composites have high-performance reinforcements of a thin diameter embedded in a matrix material such as epoxy or ceramic [1]. Even though the costs of composite materials may be higher, the fact that there are fewer components in an assembly and the cost savings from fuel make them more economical than monolithic metals. Over traditional materials, composites have a number of additional benefits, such as a better specific strength and stiffness, fatigue resistance, impact resistance, thermal conductivity or corrosion resistance, which make them suitable for those demanding applications [1–3].

The main disadvantages of composite materials for aircraft structures are their high cost of fabrication, taking into account the raw material, its processing and certification; their complex mechanical characterization in comparison with the monolithic materials, their relatively low resistance to mechanical impact and through-thickness strength due to low failure strains if the matrix is thermosetting, compared to the metal structures; they do not have neither a high combination of strength and fracture toughness nor a high strength in the out-of-plane direction. Furthermore, the shear stresses produced between the layers, particularly at the edges of the laminate, may cause delamination and the repair procedures are much more complex in comparison with the metals [1–3].

Besides that, in order to make that evolution affordable and amortisable, there is an initial investment to pay for the manufacturing processes change, the automation of the assembling lines and the development of the inspection departments, since the type of defects expected are now different and, sometimes, more difficult to detect. Repair of composites is not a simple task and critical flaws and cracks may go undetected [1, 2].

The majority of polymer matrices used in aerospace applications are epoxy-based due to their high strength, good wetting of fibres during processing and adhesion, low viscosity and low flow rates, low volatility during cure, low shrink rates, and availability in more than 20 grades to meet specific property and processing requirements [2, 3]. Limited operating temperatures, high coefficients of thermal and moisture expansion and low elastic properties in certain directions are the main limitations of polymer matrix composites. Minor epoxies are often added to the main compound in order to surpass some of those obstacles [2, 3].

Regarding the joining of composite structures, they evolved from the mechanical fastening, such as bolts and rivets, welding or soldering to more advanced technology denominated adhesive joints [4]. The adhesives are preferred to avoid the stress concentrations zones resulted from drilling operations. However, these drills are also utilised for interior access or the electronic components implementation. Their design is a very complex task, since these are often the weakest spots and there is the necessity for the connections to be reliable, distribute the load uniformly and, at the same time, be lighter [1, 4, 5]. Although the adhesive joints have better fatigue properties and less stress concentration, there are still some concerns to take into account, such as the inspection difficulties, the need for complex tools and the susceptibility to environmental degradation, due to the inevitable contact with chemical agents [1, 4, 5].

Flaws occur inevitably at composite structures, particularly between the layers and at the adhesive interfaces. They can arise either from the manufacturing process, during the ply collation, curing, adhesive bonding or machining and assembly procedures or throughout their service life. The most common are debonds, porosities, matrix cracks as manufacturing defects, and delaminations, corrosion, impact damage and fatigue during their service life [3, 6, 7]. Delamination, separation of layers resulted from loading conditions, and debond, inadvertent separation between adherends in a adhesively bonded joint during the fabrication process, are the most commonly observed failure modes among the several failure mechanisms [3, 6, 7].

There are several and strict regulations to the types and amount of damage allowed in structured materials without replacement or repair of the damaged component. Furthermore, the inhomogeneity and inherent anisotropy of composite structures make their design even further complicated, particularly for damage tolerance requirements. In order to achieve the large variety of possible defects, the aerospace industry relies on the non-destructive inspection (NDI), which is used to determine the type, size and location of damage. The main procedures range from a simple visual inspection for macroscopic flaws detection to more advanced technologies, such as ultrasonics, radiography, thermography, among others [3, 6, 8].

Nevertheless, these inspection methodologies take a lot of time, which increases substantially the total cost. Therefore, structural health monitoring techniques (SHM) are increasingly used over the time to detect defects and damage. SHM uses in situ sensor networks and intelligent data processing for continuous inspection with little or no human intervention. These sensors ought to be fairly priced, lightweight, and unobtrusive so as not to increase the structure's cost or weight or interfere with its airworthiness [6, 9]. Some examples are the conventional resistance strain gauges, which consists in the conversion between a strain change into a resistance change measured with a

precise instrument; the fiber optic sensors whose functionality is based on their optical properties or the piezoelectric-based sensors coupling the electric and mechanical variables, denominated by PWAS (piezoelectric wafer active sensor) [6, 9].

In today's engineering and, in particular, in the aerospace industry, designers have to challenge themselves in order to comply with the endless requirements, which range from the system's specifications and constrained development time to the need to establish the system's performance accurately in the first design stages.

In the aerospace industry, manufacturers create a wide range of composite structures exhibiting complex and different material behaviours as well as several designs, leading to the need of testing each one of them for validation, which is time consuming and expensive. Optimization procedures could constitute a solution, because they consider several domains and their own goals, as well as the interaction between them, that is, the goal is to find practical optimal solutions satisfying a given set of design constraints and requirements [10]. The design of aerospace systems is a multidisciplinary and complex process, which makes those procedures even more fundamental. Furthermore, composite materials offer more design variables than do metals, therefore they allow for more refined tailoring and more extensive optimization [10].

Regarding the aircraft structures, they are usually thin shell structures, whose outer surface or skin may be reinforced with longitudinal stiffening members and transverse frames to resist from bending, compressive and torsional loads without buckling. These ones are known as semi-monocoque structures. Otherwise, the monocoque structures rely exclusively in the load carrying capacity of their skin. Therefore and regardless of their construction or complexity, an aircraft structure is used to transmit and resist external loads, to provide an aerodynamic shape and to protect passengers and so forth from the environmental conditions encountered during a flight [11].

Wing structures are composed of thin skins and stiffening elements, such as stringers, spar webs and caps, and ribs. The overall structure is comprised by many cells closely spaced, which enables to assume a constant shear flow in the skin between adjacent stringers. Bending moments at any section of a wing typically result in shear loads at other sections of the wing. The ribs are transverse components which increase the column buckling stress of the longitudinal stiffeners (stringers), due to an end constraint on their column length, and the plate buckling stress of the skin panels. Ribs act as formers for the aerofoil shape at the outer zones of the wing, owing to low load levels. On the other hand, they have a robust construction closer to the wing root due to the necessity to absorb and transmit high concentrated loads derived from the undercarriage, engine thrust or fuselage attachment points reactions. In turn, the impermeable wing skin supports the aerodynamic pressure distribution capable of generating the lift necessary during a flight. Those forces are then absorbed by the ribs and stringers. Despite its high performance in resisting shear and tensile loads, wing skin generally buckles under low compressive loads, being the stiffening elements fundamental in avoiding or delaying that issue, as referred above. Regarding the spar webs, their main function is to develop shear stresses capable of resisting shear and torsional loads, performing a stabilizing function in the overall structure [11, 12].

Due to their flexibility, aircraft structures are extremely susceptible to distortion under load, which influences the aerodynamic forces and, consequently, further structural distortion is developed. Aircraft vibration may be generated by aerodynamics, mechanical issues or outside sources such as atmospheric turbulence. Every airplane has a characteristic normal vibration signature. This is a result of vibration modes at particular frequencies triggered by mass distribution and structural stiffness. Very low-level vibrations occur when the airplane is subjected to typical air-flow over its surfaces. However, the airplane's response to turbulent air is more evident and the vibration's magnitude may be greater and audibly detectable [13, 14].

Therefore, the main objectives of this work are to implement and develop an optimization framework, particularly embedded in a genetic algorithm, in an airplane wing representative structure composed of aluminium and composite materials assembled with hybrid joints, in order to achieve optimal configurations regarding the fundamental natural frequency of the structure, with the aim of avoiding an undesirable amplitude of vibration, and the maximum critical buckling load, aiming to assure the structure's safety, varying the stacking sequence, fibres' orientations and layers' thicknesses.

1.2 Optimising design for inspection

The European Cooperation in Science and Technology (COST) develops several actions, named COST actions, whose main goal is to create research networks between european scientists and, therefore, to contribute to research development and advancement. The present thesis is developed within the EU COST action CA18203, "Optimising Design for Inspection". The goal is to support the development of an integrated framework for optimised self-sensing structures capable of diagnosis and prognosis, together with demonstrators and educational activities, including training programs, which ultimately lead to cleaner and safer skies [15].

This work integrates the group responsible for establishing the design criteria based on industry needs and to analyse the requirements for integrating structural health monitoring systems (SHM) at the beginning of the design. The structure that represents the airplane wing was made available by the Cardiff School of Engineering in cooperation with the company Airbus and it is represented below, Figure 1.1.

The airplane wing representative structure is composed by two composite plates reinforced by aluminium longitudinal and transverse stiffeners. For assembling the several components, mechanical fasteners and adhesive joints are used.

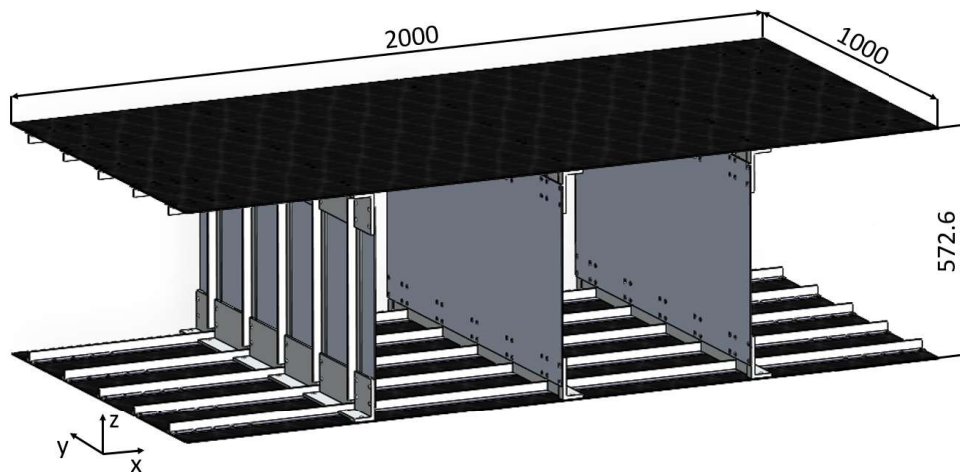


Figure 1.1 – Airplane wing representative structure. Adapted from [15].

1.3 Objectives

The main objective of this work is to implement and develop an optimization framework based on a genetic algorithm capable of predicting fibres' orientations and layers' thicknesses that maximise the fundamental natural frequency of vibration, as well as the critical buckling load due to in-plane loads. The mechanical responses are obtained using an artificial neural network (ANN) arrangement in order to reduce the computational time. Abaqus[®] software is used to provide the necessary data to train and validate the ANN.

The work plan is constituted by the following tasks:

- Understand the finite element model already implemented for the wing representative structure;
- Decompose the original optimization problem into smaller problems (substructures);
- Carry out analysis in order to maximise the first natural frequency of vibration;
- Carry out analyses in order to maximise the critical buckling load due to in-plane loads;
- Carry out a multi-objective optimization regarding the critical buckling load and weight of the structure due to in-plane loads;
- Development of an analytical first approach to validate the FEM model used to obtain the fundamental natural frequency of a stiffened composite panel;
- Compare the diverse optimum designs.

1.4 Thesis layout

The work developed is divided into the following chapters:

- Chapter 1: "Introduction", in which the main motivations for the realization of this dissertation are presented coupled with its applicability on the aerospace industry nowadays;
- Chapter 2: "State of the art", wherein the principal optimization procedures are reviewed and assessed upon their possible application in this concrete problem. The genetic algorithm capable of optimising the ANN arrangement and the mechanical variables under consideration is deeply analysed;
- Chapter 3: "Mathematical model". In this section, the main equations regarding the composite laminates behaviour are formulated, particularly their performance under free conditions and in-plane loads;
- Chapter 4: "Wing representative structure's description", in which the complete description of the structure under analysis is performed, including its main parts and the respective mechanical properties. Besides that, the peculiarities of the implemented FEM models are discussed (e.g. type of elements);
- Chapter 5: "Optimization of the airplane wing representative structure for vibration". In this chapter, the simplified structure is optimised regarding its fundamental natural frequency, under certain prescribed constraints and altering only the layers' orientations and/or thicknesses. The thorough description of the optimization algorithm is provided;
- Chapter 6: "Optimization of the airplane wing representative structure for buckling". The same procedure described in the previous chapter is implemented to maximise the structure's critical buckling load due to in-plane loads, considering the plies' orientations and layers' thicknesses as design variables. The aggregation method is used to take into account the minimisation of the structure's weight as an additional goal;
- Chapter 7: "Conclusions and future work", wherein the main conclusions about the developed work are synthesised and a perspective of future work regarding possible improvements on the optimization procedure are drawn.